Delia Volpi

Dipartimento di Astronomia e Scienza dello Spazio-Università degli Studi di Firenze-Italia

Simulated synchrotron emission from Pulsar Wind Nebulae

In collaboration with:

Luca Del Zanna-Dipartimento di Astronomia e Scienza dello Spazio-Università degli Studi di Firenze-Italia

Elena Amato-INAF-Osservatorio Astrofisico di Arcetri-Firenze-Italia

Niccolò Bucciantini-Astronomy Department-University of California at Berkeley-USA

Abstract

Basing on the set of MHD equations and the evolution equation of the maximum energy of the emitting particles (which includes adiabatic and synchrotron losses along streamlines) a complete set of diagnostic tools aimed at producing synthetic synchrotron emissivity, polarization and spectral index maps from relativistic MHD simulation is obtained.
A first application of this method is the emission from Pulsar Wind Nebulae (PWNe).
The employed numerical code is described in Del Zanna & Bucciantini (2002), Del Zanna et al. (2003) and Londrillo & Del Zanna (2004).
It is a shock-capturing code solving the ideal relativistic MHD and energy evolution equations in conservative form.
Axisymmetric simulations of PWNe are directly compared with the observations of the inner structure of Crab Nebula and similar objects in the optical and X-ray bands. The typical observed PWNe jet-torus morphology is well reproduced even in the finer emission details (arcs, rings and the bright knot) and in the velocity ranges. Spectral properties (spectral index maps and integrated spectra) are also, partially, reproduced.
Further details can be found in Bucciantini et al. (2005) and Del Zanna et al. (2006).

Introduction

- Optical and X-ray observations at high resolution from space (Hubble, ROSAT, Chandra, XMM-Newton) show a jet-torus structure in Pulsar Wind Nebulae (PWNe, e.g. Crab Nebula and Vela).

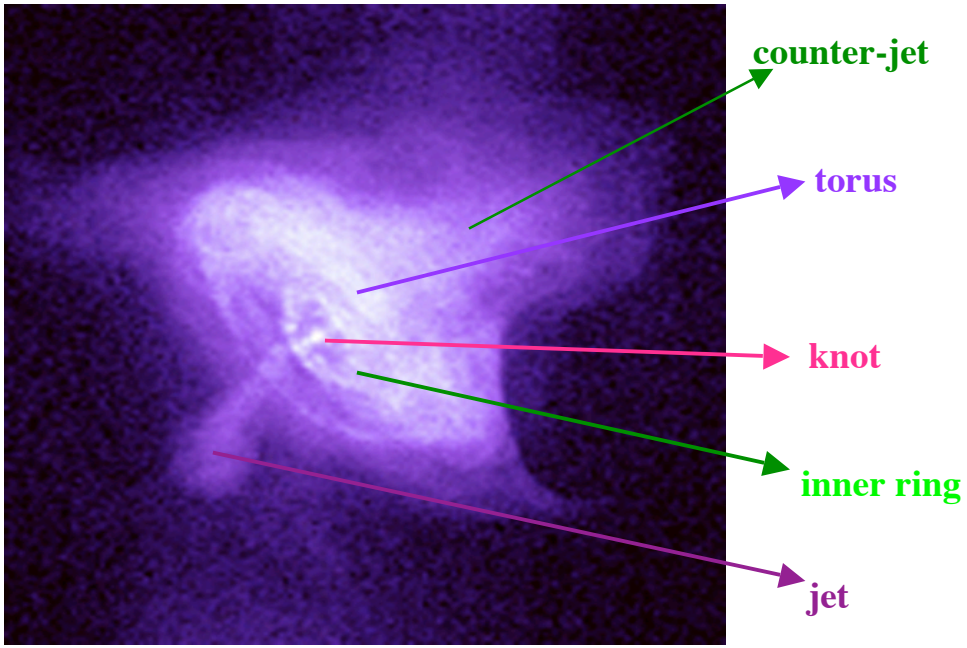

Crab Nebula (Chandra, X-ray)

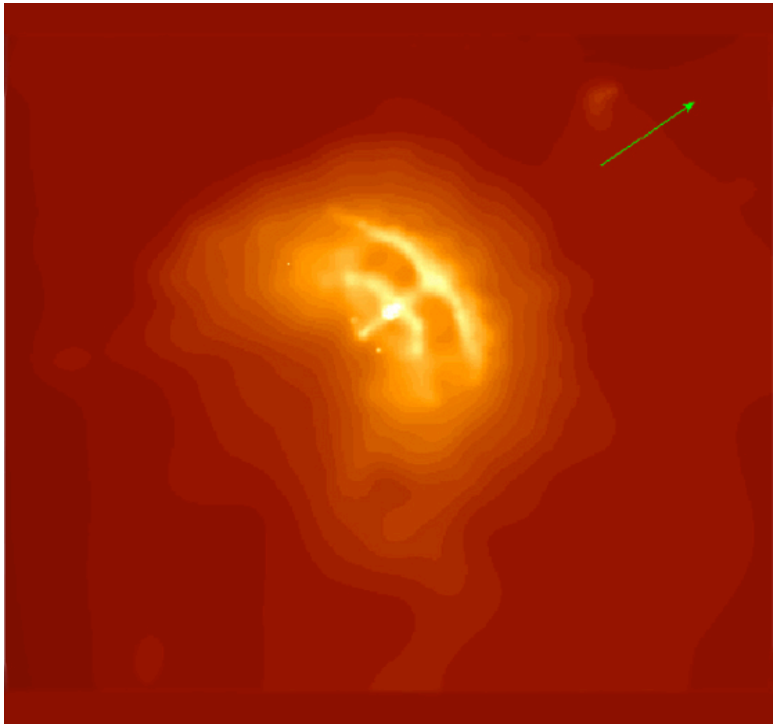

Vela (Chandra, X-ray)

PWNe is a class of Supernova Remnants (SNR) called plerions. Plerions are hot bubbles emitting non-thermal radiation (synchrotron and Inverse Compton) at all wavelenghts and receiving relativistic particles and magnetic field from the engine-pulsar. They are created by interaction between ultra-relativistic magnetized pulsar wind (PW) and espanding SNR ejecta.

Introduction

• The scheme of a plerion is (Kennel and Coroniti, 1984):

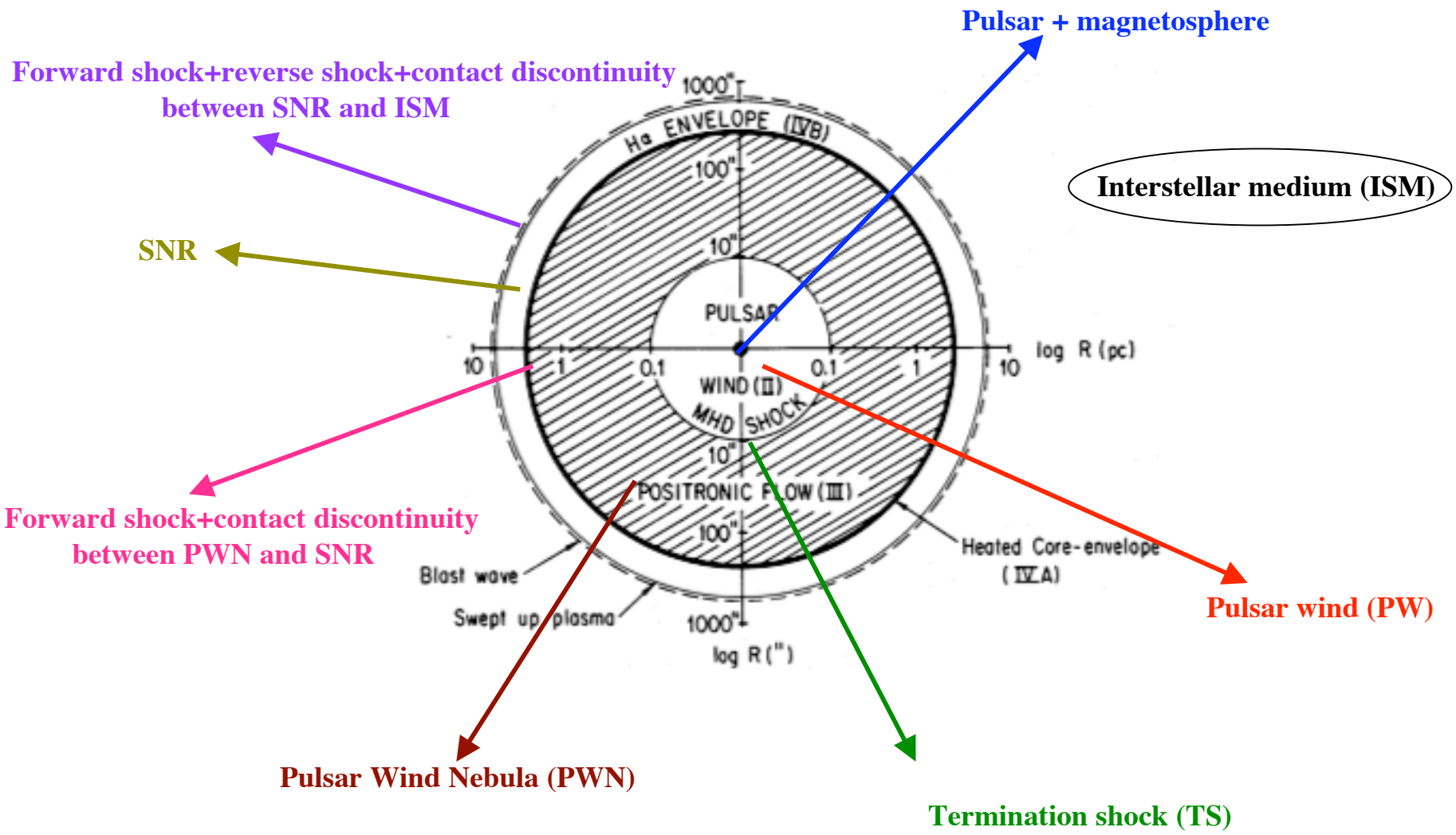

Introduction

- Pulsar spin-down energy is converted to Poynting flux (mainly a toroidal field) and in pair wind ($\sigma >> 1$). At termination shock (TS) models predict $\sigma << 1$ to reproduce observed synchrotron emission: **sigma paradox**. Around the equator there is a striped wind region where magnetic field B may decrease because of equatorial reconnection.
(figure from Coroniti, 1990)

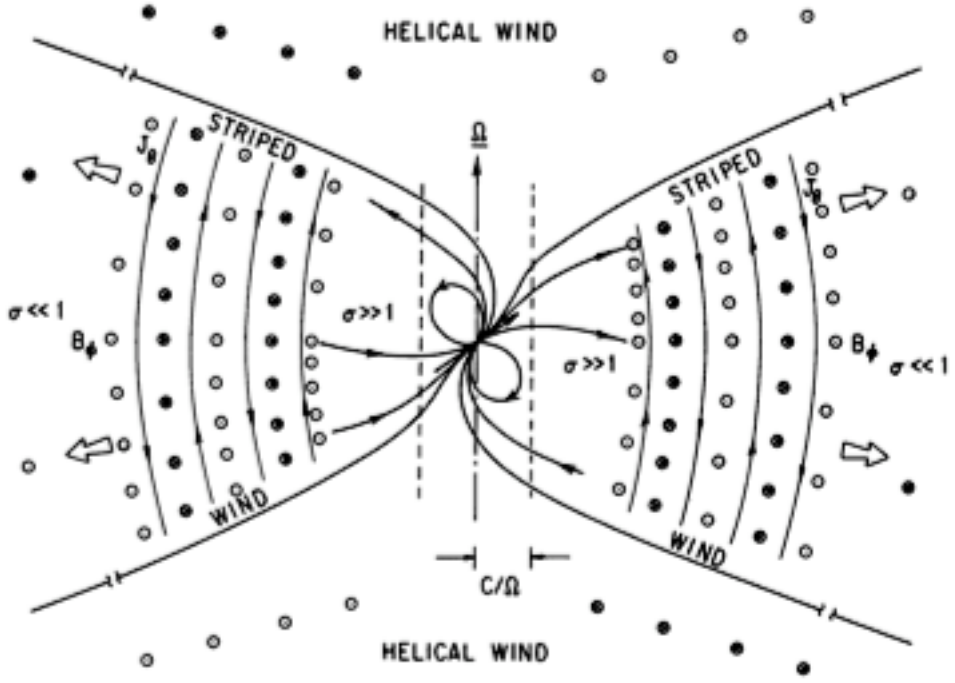

Introduction

•1-D RMHD theoretical models (Kennel & Coroniti, 1984-- Emmering & Chevalier, 1987) can explain torus, but not jets. 2-D theoretical ones (Bogovalov & Khangoulian, 2002 -- Lyubarsky, 2002) try to interprete jet-torus morphology. The idea is: an anisotropic flux energy (stronger at the equator) create torus and TS oblate shape; jets are collimated downward TS (where flux is only mildly relativistic) and appear originate from the pulsar because of the cusp in TS.

(Lyubarsky, 2001)

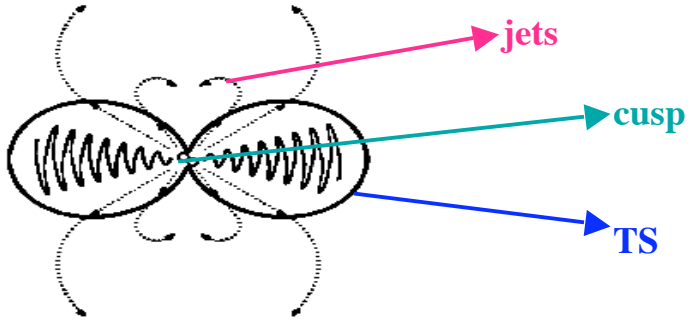

- Only with developments of shock - capturing RMHD numerical scheme (Komissarov, 1999 -- Del Zanna et al., 2003) has been possible to solve hyperbolic equations and confirm theories about jet-torus morphology.
- Initially theoretical formulas and numerical recipes (used in the code to solve the problem of the jet-torus structure) are presented. Then simulation maps are shown and discuss to understand dynamics and radiative emission of PWNe. At the end there will be results and future developments.
- *This work represents a complete set of diagnostic tools aimed at producing synchrotron emissivity, polarization and spectral index maps from RMHD simulations not only for PWNe, but also for the study of different classes of objects (e.g. AGN jets).*

Synchrotron emission recipes

- Emitting particles' isotropic distribution function at termination shock (TS = 0) (Kennel & Coroniti, 1984b):

$$f_0(\varepsilon_0) = \frac{A}{4\pi}\varepsilon_0^{-(2\alpha+1)} \qquad \varepsilon_0^{\min} \le \varepsilon_0 \le \varepsilon_0^{\max} \qquad A = K_n n_0 = K_p \frac{p_0}{mc^2}$$

particle Lorentz factor

spectral index

- Time evolution of single energies along post-shock streamlines in comoving frame (‘):

$$\frac{d}{dt'}\ln\varepsilon = \frac{d}{dt'}\ln n^{1/3} + \frac{1}{\varepsilon}\left(\frac{d\varepsilon}{dt'}\right)_{sync} \qquad \left(\frac{d\varepsilon}{dt'}\right)_{sync} = -\frac{4e^4}{9m^3c^5}B'^2\varepsilon^2$$

adiabatic losses

synchrotron losses averaged with pitch angles

This equation is evolved in conservative form for ε_∞ (maximum particle energy = particle remaining energy with $\varepsilon_0 \to \infty$).

- Post-shock distribution function (obtained from conservation of particles'number along streamlines and under condition of $\alpha \approx 0.5$):

$$f(\varepsilon) = \frac{K_p}{4\pi}\frac{p}{mc^2}\varepsilon^{-(2\alpha+1)} \qquad \varepsilon < \varepsilon_\infty \qquad K_p = \text{constant}$$

Synchrotron emission recipes

- Emission coefficient in observer's fixed frame:

$$j_\nu(\nu,\hat{n}) \propto Cp\left|\vec{B}' \times \hat{n}'\right|^{\alpha+1} D^{\alpha+2}\nu^{-\alpha} \qquad \nu_\infty \geq \nu$$

$$j_\nu(\nu,\hat{n}) = 0 \qquad \nu_\infty < \nu$$

optical or X-ray frequency of observation

Relativistic corrections:

$$D = \frac{1}{\gamma(1-\vec{\beta}\bullet\hat{n})} = \text{Doppler boosting factor} \qquad \vec{\beta} = \frac{\vec{\mathrm{v}}}{\mathrm{c}}$$

$$\hat{\mathrm{n}}' = D\left[\hat{n} + \left(\frac{\gamma^2}{\gamma+1}\vec{\beta}\bullet\hat{n} - \gamma\right)\vec{\beta}\right] \qquad \vec{B}' = \frac{1}{\gamma}\left[\vec{B} + \frac{\gamma^2}{\gamma+1}(\vec{\beta}\bullet\vec{B})\vec{\beta}\right]$$

observer direction versor

- Cut-off frequency for synchrotron burn-off (evolved in the code from the maximum particle energy):

$$\nu_\infty = D\frac{3e}{4\pi mc}\left|\vec{B}' \times \hat{n}'\right|\varepsilon_\infty^{\ 2}$$

Synchrotron emission recipes

- Surface brightness:

$$I_\nu(\nu,Y,Z)=\int_{-\infty}^{+\infty} j_\nu(\nu,X,Y,Z)\,dX \qquad \text{X = line of sight} \qquad \text{Y,Z = plane of sky}$$

- Stokes parameters (linear polarization):

$$Q_\nu(\nu,Y,Z)=\frac{\alpha+1}{\alpha+5/3}\int_{-\infty}^{+\infty} j_\nu(\nu,X,Y,Z)\cos(2\chi)\,dX$$

$$U_\nu(\nu,Y,Z)=\frac{\alpha+1}{\alpha+5/3}\int_{-\infty}^{+\infty} j_\nu(\nu,X,Y,Z)\sin(2\chi)\,dX$$

local polarization position angle between emitted electric field and Z

- Polarization fraction (Π) and polarization direction (**P**):

$$\Pi_\nu=\frac{\sqrt{Q_\nu^{\,2}+U_\nu^{\,2}}}{I_\nu} \qquad \vec{P}_\nu=\Pi_\nu\left(\sin(\chi)\hat{x}+\cos(\chi)\hat{y}\right)$$

- Spectral index (α_ν) for two frequencies (ν_1, ν_2) and integrated spectra (F_ν):

$$\alpha_\nu(\nu_1,\nu_2,Y,Z)=-\frac{\log\left[I_\nu(\nu_2,Y,Z)/I_\nu(\nu_1,Y,Z)\right]}{\log(\nu_2/\nu_1)}$$

$$F_\nu(\nu)=\frac{1}{d^2}\iint I_\nu(\nu,Y,Z)\,dY\,dZ$$

d=distance of emitting object

Numerical recipes

- Shock capturing code (Del Zanna et al., 2002, 2003, 2004)
- Ideal 2-D (axisymmetry) RMHD equations (with adiabatic equation of state and $\vec{E} = -\vec{v} \times \vec{B}$) and equation of the maximum energy in conservative form are evolved in time and space
- **B** toroidal, **v** poloidal
- Spherical coordinates: r, θ
- **Initial cold ultrarelativistic Pulsar Wind conditions (0 = equator)**:

  Lorentz factor (conservation of energy along streamlines) :

  $$\gamma(\theta) = \gamma_0\left(\alpha_0 + (1-\alpha_0)\sin^2\theta\right) \qquad \gamma_0 = 100 \quad \alpha_0 = 0.1 \quad \text{anisotropy parameter}$$

  Anisotropic energy flux:

  $$F_0(r,\theta) = F_0\left(\frac{r_0}{r}\right)^2\left[\alpha_0 + (1-\alpha_0+\sigma)\sin^2\theta\right] \qquad \sigma = \frac{B^2}{4\pi w\gamma^2} = \text{magnetization parameter}$$

  $(b\to\infty \quad \theta=\pi/2)$

  $w=\rho c^2+4p$

  Toroidal field:

  $$B(r,\theta) = B_0\left(\frac{r_0}{r}\right)\sin\theta\tanh\left[b\left(\frac{\pi}{2}-\theta\right)\right] \qquad b = \text{width of striped wind region}$$

  toroidal B and unmagnetized equatorial region

  v radial, $\rho \propto r^{-2}$
- Supernova Remnants + Interstellar Medium
- **Runs with $\sigma_{effective}$=0.02 (averaged over θ): A (σ=0.025, b=10) B (σ=0.1, b=1)**

Wind magnetization

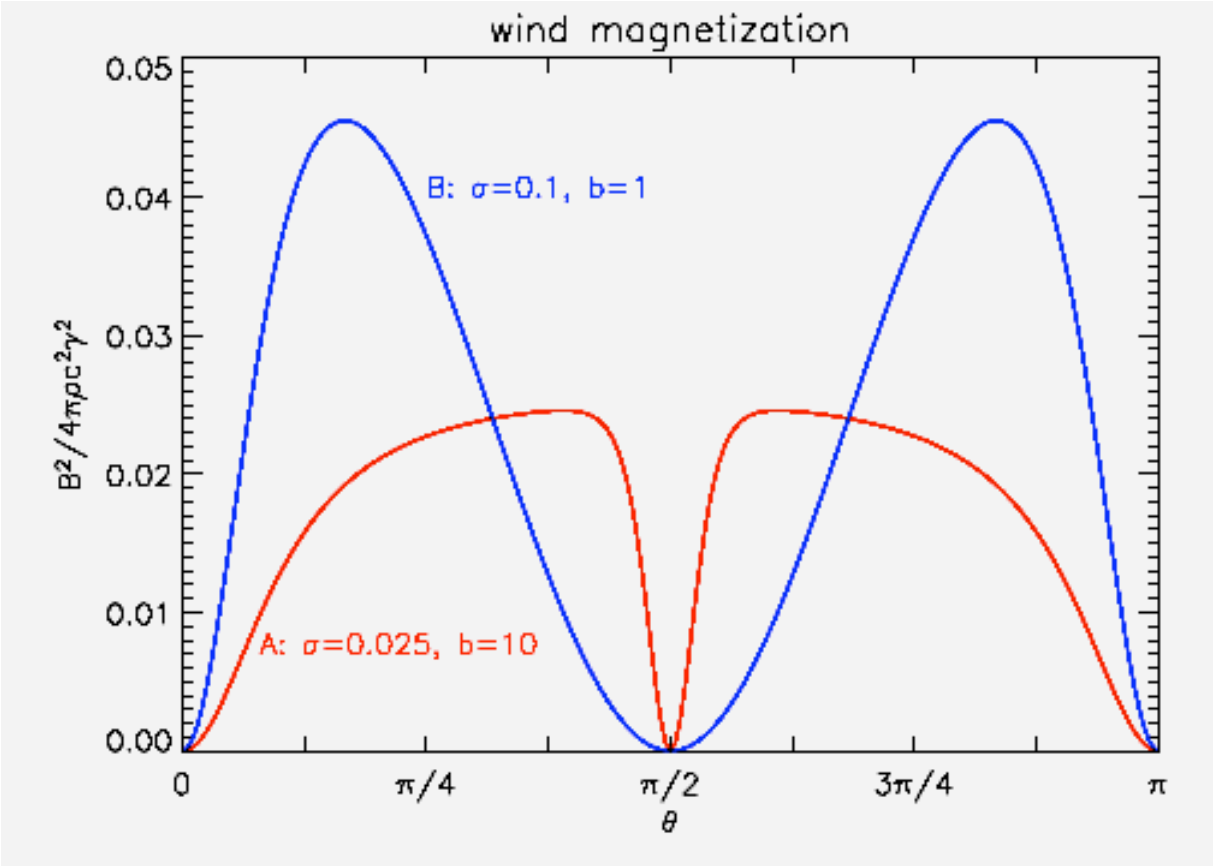

Results: flow structure maps

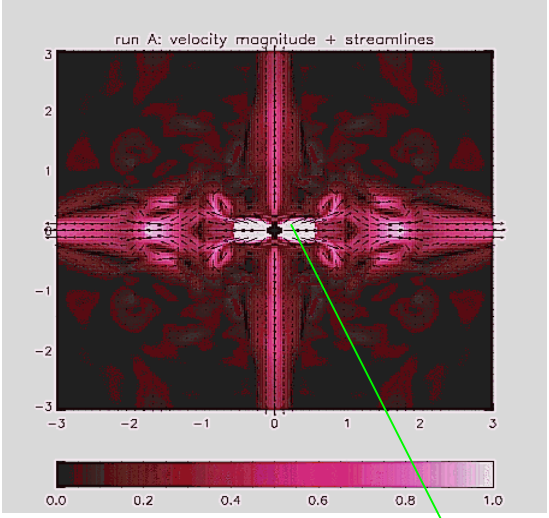

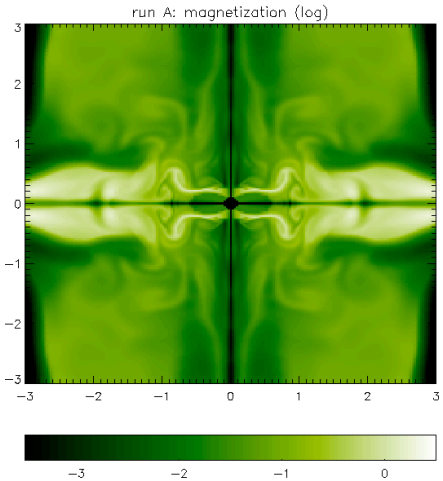

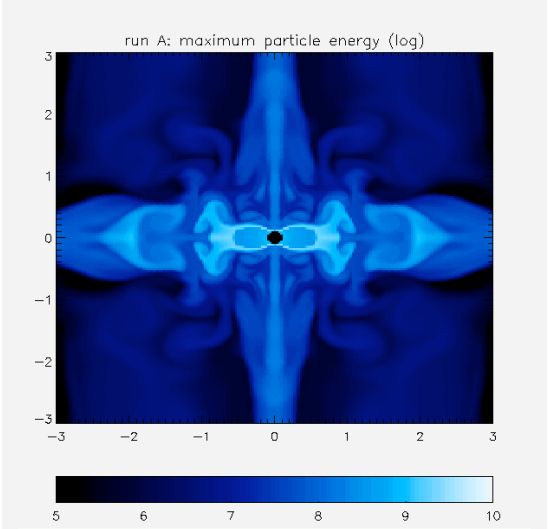

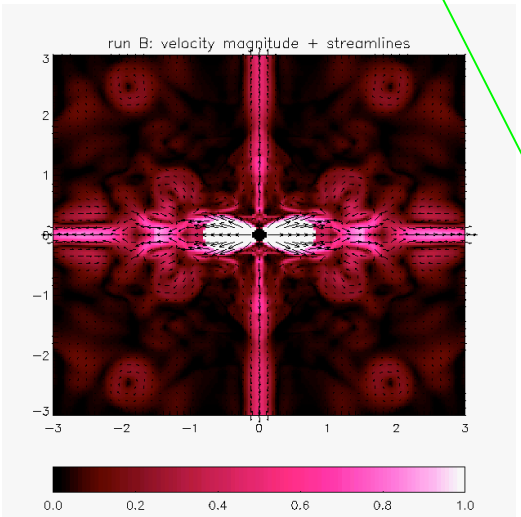

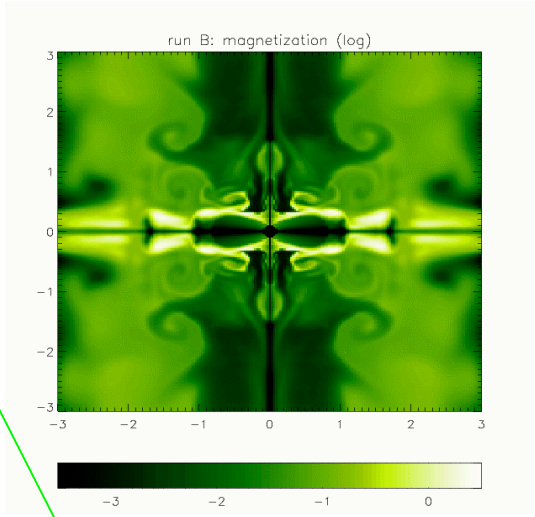

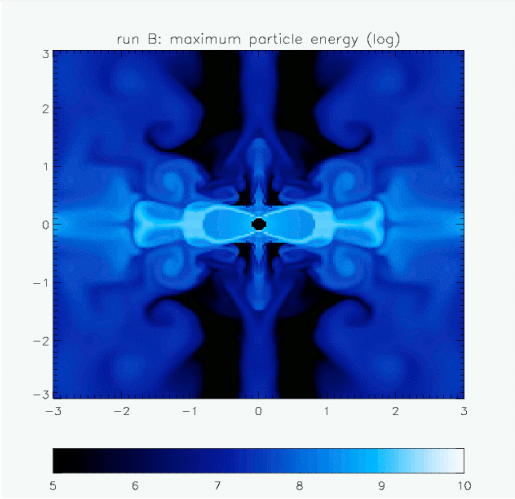

- RunA: a) Stronger pinching forces ⇒ smaller wind zone; b) Equipartition near TS; c) Larger magnetized region ⇒ particles loose most of their energy nearer to TS; d) Less complex magnetization map.
- Supersonic jets and equatorial outflow: v ≈ 0.5-0.7c (as in Crab Nebula-Hester-2002, Vela-Pavlov 2003).

Results: surface brightness maps

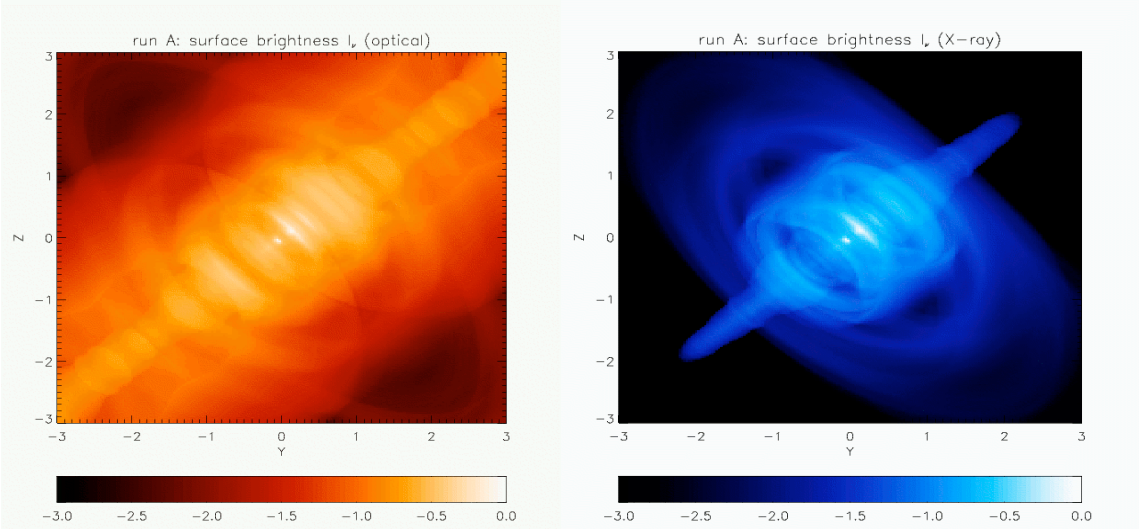

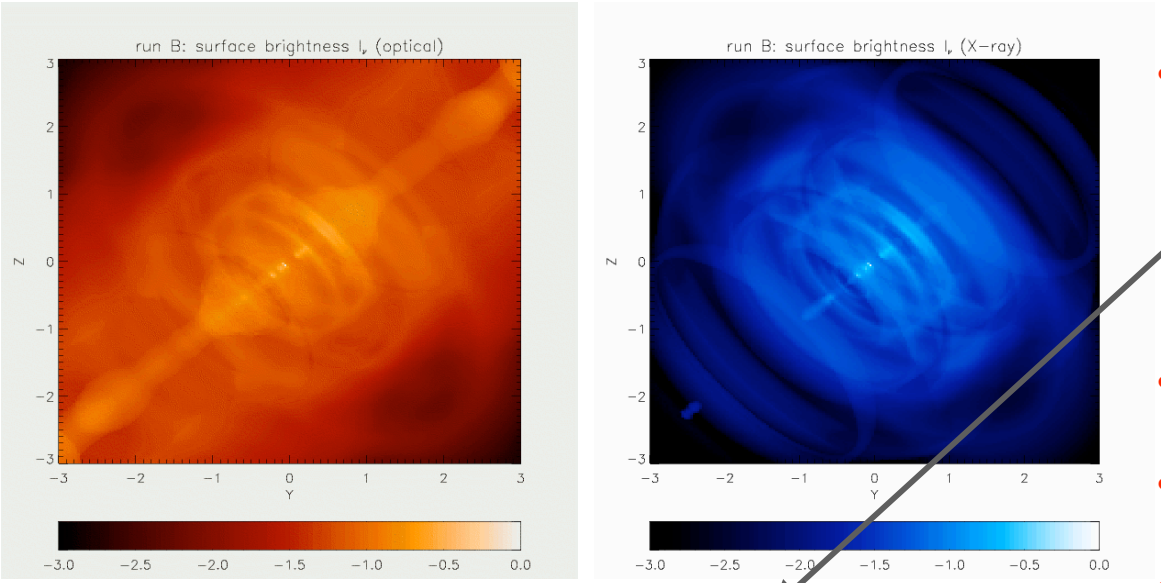

All values are Crab Nebula ones

- Optical and X emitting particles: $\alpha_\nu = 0.6$ (Veron-Cetty & Woltjer, 1993)
- Cut-off frequencies: $\lambda = 5364$ Å in optical maps (V.C.,1993) $h\nu = 1$keV in X maps (Chandra)
- Angles (Weisskopf, 2000): inclination of symmetry axis: 30^0 rotation respect to North: 48^0
- I_ν normalized respect to maximum value, logarithmic scales
- Larger emitting regions in optical than in X band⇒synchrotron burn-off
- Internal regions: system of rings (connected to external vortices), brighter arch (inner ring), a central knot (connected to polar cusp region) due to Doppler boosting (very strong near TS, $v \approx c$)
- Stronger emission near TS where magnetization and velocity are higher
- RunA is similar to Crab Nebula, (stronger synchrotron losses)
- RunB is similar to Vela (lower magnetization around equator)

Results: optical polarization maps

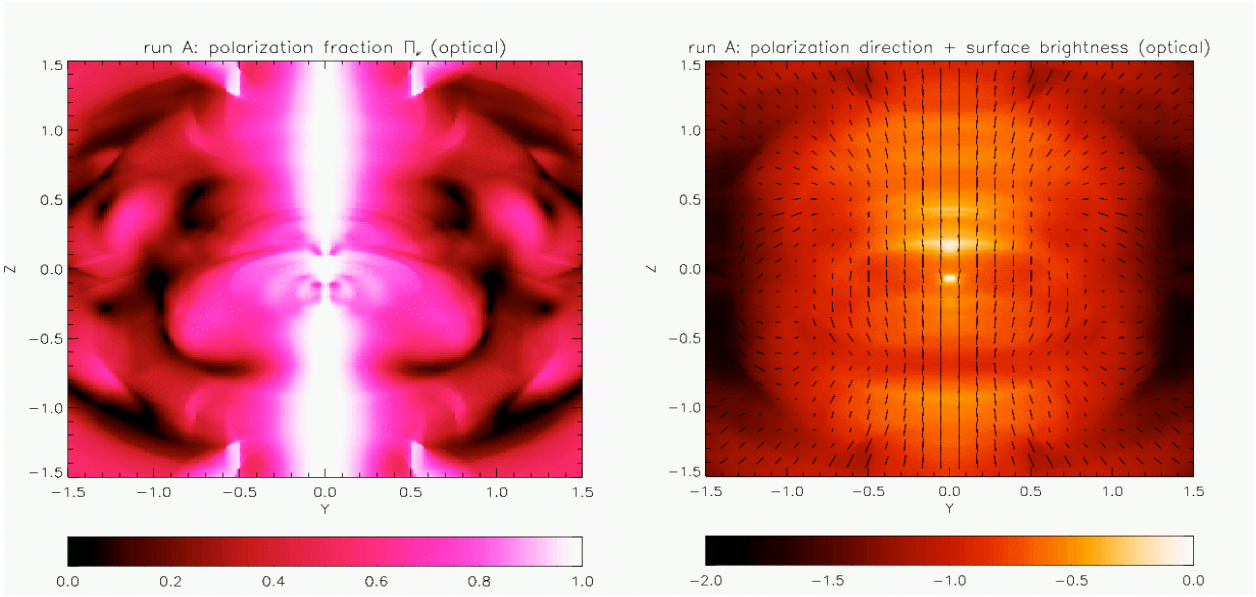

- Synchrotron emission ⇒ linear polarization

  Polarization fraction

- Polarization fraction is normalized against $(\alpha_\nu+1)/(\alpha_\nu+5/3)\approx 70\%$
- Along polar axis: higher polarized fraction (projected B ⊥ line of sight)
- Outer regions: depolarization (due to opposite signs of projected B contributions along line of sight)

  Polarization direction

- Polarization ticks are basically ortogonal to B, their lenght is proportional to polarization fraction
- Polarization angle swing (deviation of vector direction) in brighter arcs where $v \approx c$ and Doppler boost is stronger
- RunB: more complex structure

Results: spectral index maps

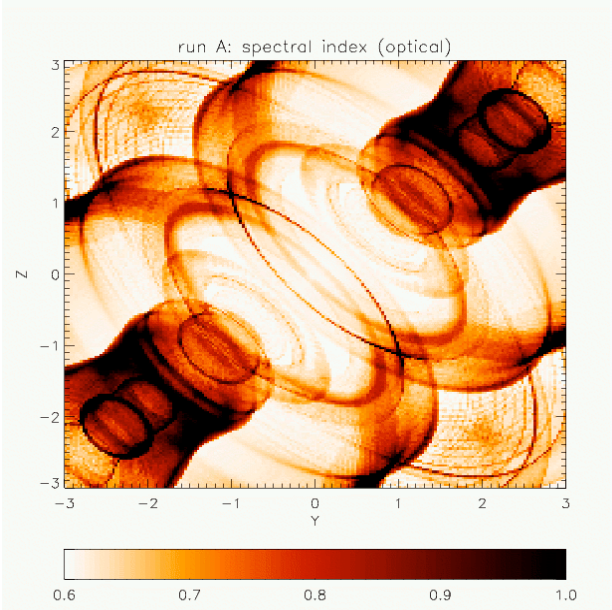

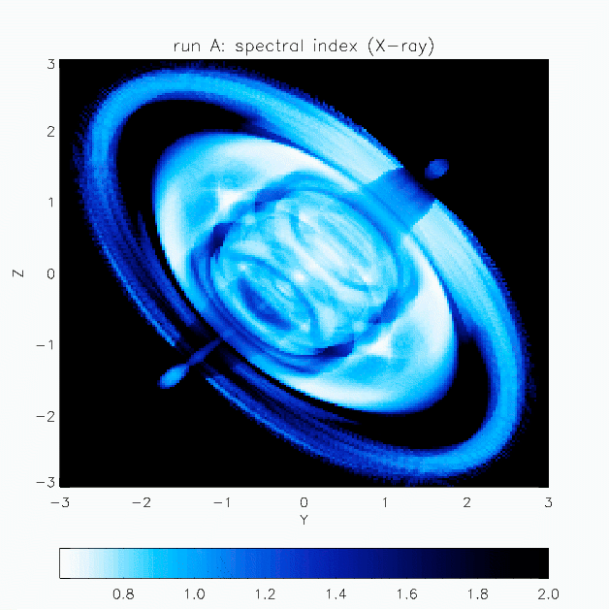

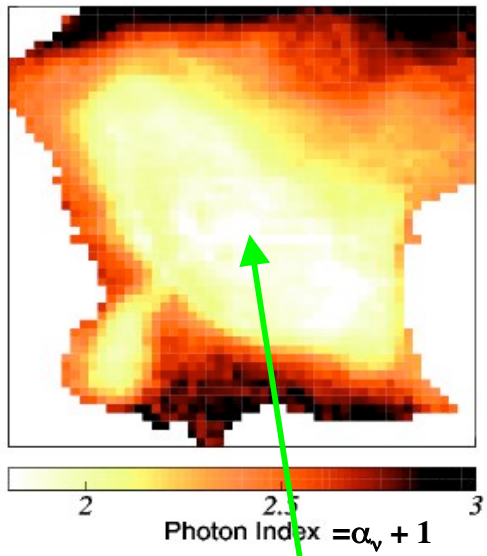

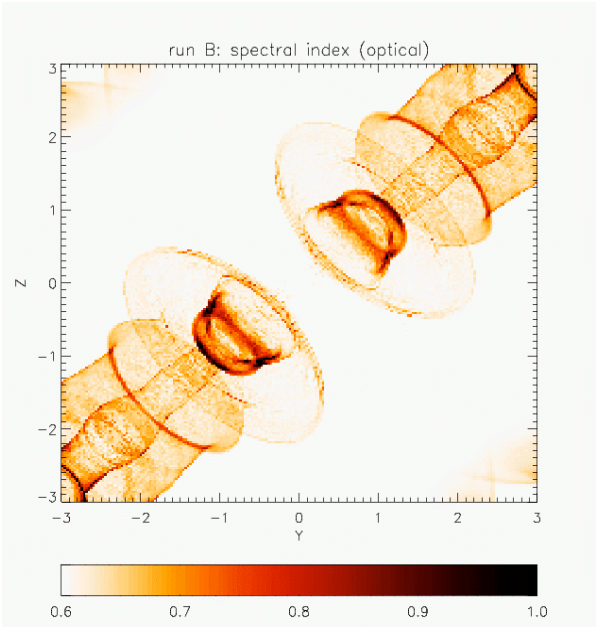

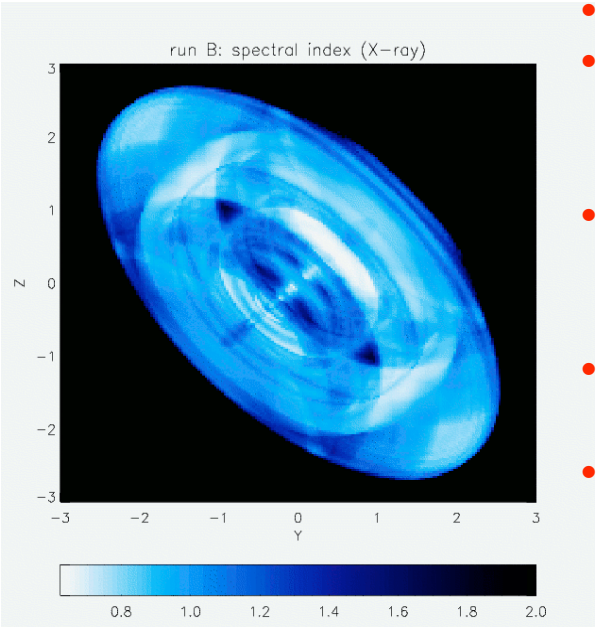

- Values of Crab Nebula
- Optical maps obtained with: λ_1=5364Å, λ_2=9241Å (Veron-Cetty & Woltjer, 1993)
- X-ray maps obtained with: $h\nu_1$=0.5keV, $h\nu_2$=8keV (Mori et al., 2004)
- Spectral index grows from inner to outer regions
- RunA: X-ray simulated spectral index maps similar to ones of Crab Nebula (Mori et al, 2004)

Conclusions

- The present work confirm jet-launching mechanism due to magnetic hoop-stresses.
- For the first time a complete set for calculating simulated optical and X-ray synchrotron emission, polarization and spectral index maps are produced accounting for synchrotron losses.
- There is a good agreement between maps of runs and observations (especially between maps of RunA and Crab images and between maps of RunB and Vela images).
  In fact velocity magnitude maps present the same observed range of values along the polar jets and the equatorial outflow.
  The brightness maps present the same observed features (equatorial torus, jet and counter-jet, inner ring, brighter arcs and a central knot) even in the details .
  Spectral index maps are similar to the observed ones by Veron-Cetty & Woltjer (1993) for optical band and by Mori et al. (2004) for X-ray band.
- An estimation of pulsar wind parameters is done: σ (magnetization parameter) and b (width of the equatorial striped region connected to the angle between the pulsar rotation and magnetospheric axes) with $\sigma_{effective} > 0.01$ to have supersonic polar jets.
- Future: further optimization of the model parameters; higher temporal and spatial resolution; 3-D simulations for reproducing magnetic reconnection and MHD instabilities (kinks in jets).

References

- Jet-torus in PWNe:synchrotron and polarization maps

  L. Del Zanna, D. Volpi, E. Amato, N. Bucciantini, **A&A**, 2006, vol.453, p.621-633
  N. Bucciantini, L. Del Zanna, E. Amato, D. Volpi, **A&A**, 2005, vol.443, p.519-524
- Bow-shock PWNe

  N. Bucciantini, E. Amato, L. Del Zanna, **A&A,** 2005, vol.434, p. 189-199
- Rayleigh Taylor instabilities (filaments)

  N. Bucciantini, E. Amato, R. Bandiera, J. M. Blondin, L. Del Zanna, **A&A**, 2004, vol. 423, p.253-265
- Kelvin-Helmholtz instability: synchrotron modulation in PWNe

  N. Bucciantini, L. Del Zanna, astro-ph/0603481, 2006
- 2-D PWN-SNR simulations: jet-torus structure

  L. Del Zanna, E. Amato, N. Bucciantini, **A&A**, 2004, vol.421, p. 1063-1073

References

- 1-D PWN-SNR simulations

  N. Bucciantini, R. Bandiera, J. M. Blondin, E. Amato, L. Del Zanna, **A&A**, 2004, vol. 422, p. 609-619

  N. Bucciantini, J. M. Blondin, L. Del Zanna, E. Amato, **A&A**, 2003, vol. 405, p. 617-626
- Neutron stars: relativistic MHD wind

  N. Bucciantini, T. A. Thompson, J. Arons, E. Quataert, L. Del Zanna, **MNRAS**, 2006, vol. 368, p. 1717-1734
- RHD and RMHD numerical code

  L. Del Zanna, N. Bucciantini, P. Londrillo, **A&A**, 2003, vol. 400, p. 397-413

  L. Del Zanna, N. Bucciantini, **A&A**, 2002, vol. 390, p.1177-1186